

Probing nucleation, reverse annealing, and chaperone function along the reaction path of HIV-1 single-strand transfer

Yining Zeng*, Hsiao-Wei Liu*, Christy F. Landes*, Yoen Joo Kim*, Xiaojing Ma*, Yongjin Zhu*, Karin Musier-Forsyth[†], and Paul F. Barbara**

*Center for Nano and Molecular Science and Technology, University of Texas, Austin, TX 78712; and [†]Department of Chemistry, Ohio State University, Columbus, OH 43210

Edited by Robert J. Silbey, Massachusetts Institute of Technology, Cambridge, MA, and approved May 16, 2007 (received for review January 12, 2007)

Reverse transcription of the HIV-1 genome involves several nucleic acid rearrangement steps that are catalyzed (chaperoned) by the nucleocapsid protein (NC), including the annealing of the transactivation response region (TAR) RNA of the genome to the complementary sequence (TAR DNA) in minus-strand strong-stop DNA. It has been extremely challenging to obtain unambiguous mechanistic details on the annealing process at the molecular level because of the kinetic involvement of a complex and heterogeneous set of nucleic acid/protein complexes of variable structure and variable composition. Here, we investigate the *in vitro* annealing mechanism using a multistep single-molecule spectroscopy kinetic method. In this approach, an immobilized hairpin is exposed to a multistep programmed concentration sequence of NC, model complementary targeted-oligonucleotides, and buffer-only solutions. The sequence controllably “drags” single immobilized TAR hairpins among the kinetic stable states of the reaction mechanism; i.e., reactants, intermediates, and products. This single-molecule spectroscopy method directly probes kinetic reversibility and the chaperone (catalytic) role of NC at various stages along the reaction sequence, giving access to previously inaccessible kinetic processes and rate constants. By employing target oligonucleotides for specific TAR regions, we kinetically trap and investigate structural models for putative nucleation complexes for the annealing process. The new results lead to a more complete and detailed understanding of the ability of NC to promote nucleic acid/nucleic acid rearrangement processes. This includes information on the ability of NC to chaperone “reverse annealing” in single-strand transfer and the first observation of partially annealed, conformational substates in the annealing mechanism.

HIV-1 nucleocapsid protein | transactivation response element

Reverse transcription of the HIV-1 RNA genome involves several critical nucleic acid rearrangement steps that are chaperoned (catalyzed) by the HIV-1 nucleocapsid protein, NC (1, 2). Mechanistic investigations of these rearrangements have been challenging because of the extreme structural and kinetic heterogeneity of these processes, which are believed to involve a heterogeneous distribution of nucleic acid/protein complexes of variable composition and unknown secondary structure (3). These challenges have been particularly well documented for the NC annealing of the transactivation response region (TAR) RNA of the HIV-1 genome to the complementary sequence (TAR DNA) in minus-strand strong-stop DNA (4). Liu *et al.* (5) recently investigated the kinetics of an *in vitro* model (equation *i* of Fig. 1) for this multistep reaction; i.e., the annealing of two hairpins to produce the thermodynamically favored duplex. In the experiments of Liu *et al.*, isolated TAR hairpins were immobilized on a biologically compatibilized coverslip that was located within a flow system that supplied “fresh” unaggregated solution of complementary DNA or RNA hairpin. Real-time fluorescence single-molecule spectroscopy (SMS) of oligonucleotides labeled with donor (D) and acceptor (A) dyes was used to

simultaneously monitor the annealing kinetics, the secondary structure of the reactants, and the state-of-aggregation of the hairpins, *in situ*. Internal distances between labeled sites in reacting hairpin pairs were probed by time-resolved fluorescence resonance energy transfer (i.e., single-molecule FRET) between the donor and acceptor dyes.

Based on the data of Liu *et al.* (5) and previous observations, these authors proposed a hypothetical mechanism for the annealing reaction that is summarized by equations *ii* and *iii* of Fig. 1. The reacting hairpins in this mechanism undergo a rapid NC-induced equilibrium between closed and partially melted “Y”-shaped conformations, which is supported by previous experiments (6, 7). The chaperone (catalytic) activity of NC is envisioned as arising from essentially two independent effects: an NC-induced partial melting of the Watson–Crick pairing of the reactant hairpins (8–11) and an NC-induced decrease in the energy cost of bringing the hairpins together to form the encounter complex, due presumably to a screening of the negative charges on the hairpins and perhaps through specific interactions (12–16). The nucleation of annealing occurs in an encounter complex that is comprised of partially melted TAR DNA and TAR RNA hairpins and several bound molecules of NC (5). Two nucleation-complex isomers are envisioned for the annealing process, depending on whether the annealing occurs in the region of the L1L2 internal loops or, alternatively, in the region of the L4 internal bulge and hairpin loop (HL) of TAR DNA. The L1~L4 and HL regions are indicated in equation *i* of Fig. 1.

Here, the annealing reaction between TAR DNA and various DNA or RNA oligonucleotides (Fig. 2) is probed by a new SMS approach in which single-molecule kinetic data are acquired while the immobilized TAR DNA hairpins are exposed to a time-programmed concentration sequence of different targeted oligonucleotides with and without the NC chaperone present in the solution. This procedure chemically “drags” individual pairs of reacting hairpins through the reactant states and the intermediate states, and back again (5). This approach offers information on the different stages of the annealing mechanism, especially the putative nucleation complexes. The experiments described in this article have been built on previous simpler SMS TAR DNA annealing studies with DNA oligonucleotides (5).

Author contributions: P.F.B. designed research; Y. Zeng, H.-W.L., C.F.L., Y.J.K., X.M., and Y. Zhu performed research; K.M.-F. contributed new reagents/analytic tools; Y. Zeng, H.-W.L., C.F.L., Y.J.K., X.M., and Y. Zhu analyzed data; and P.F.B. wrote the paper.

The authors declare no conflict of interest.

This article is a PNAS Direct Submission.

Abbreviations: cTAR, complementary TAR; SMS, single-molecule spectroscopy; TAR, transactivation response element.

[†]To whom correspondence should be addressed. E-mail: p.barbara@mail.utexas.edu.

© 2007 by The National Academy of Sciences of the USA

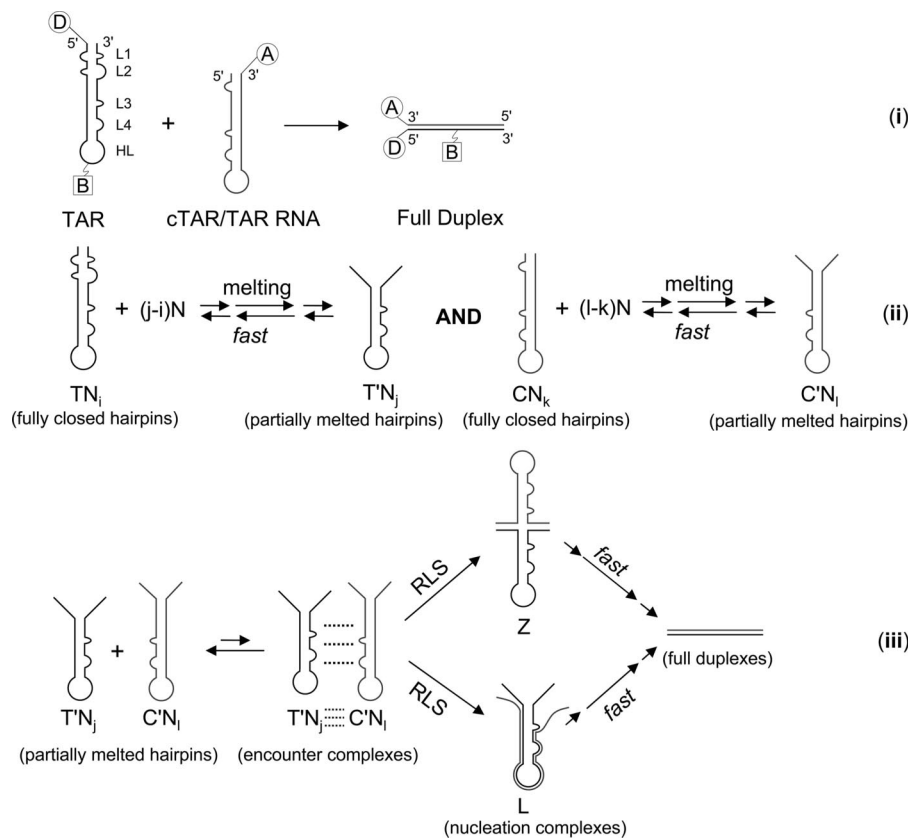


Fig. 1. Hypothetical kinetic scheme for NC-chaperoned annealing of Cy3-labeled TAR DNA to its Cy5-labeled complements, with Cy3 as fluorescence donor (D) and Cy5 as acceptor (A). T, TAR DNA; C, complementary cTAR DNA or TAR RNA; N, nucleocapsid protein, NC. In this scheme, N binds to T and C, leading to a partially melted structure, namely the Y form of T (T') and C (C'). The subscripts i , j , k , and l are used to describe the number of NC bound to nucleotides. Two partially melted hairpins form an encounter complex that leads to the formation of nucleation complexes. The annealing can go through either zipper nucleation or loop nucleation, therefore forming zipper nucleation complexes (Z) or loop nucleation complexes (L), both leading to the formation of fully annealed duplexes.

Results and Discussion

The multicomponent, oligonucleotide SMS experiments that are the focus of this article can be put in context by first considering the previously investigated annealing of “full-length” hairpin complementary TAR (cTAR) DNA to an immobilized TAR-DNA hairpin (equation i of Fig. 1) (5, 17). Single-molecule kinetic results for this reaction are shown in the first column of Fig. 3. Here, the irreversible NC-catalyzed annealing reaction was initiated by exposing a dilute, immobilized sample of the Cy3-TAR DNA to a freshly mixed solution of Cy5-cTAR DNA and NC at zero time, $t = 0$, in analogy to a stopped-flow experiment. The freshly mixed solution was prepared *in situ* in a mixing chamber that combined various concentrations of acceptor-labeled short oligonucleotides solutions in Hepes buffer and a 889 nM solution of NC. Before $t = 0$, only a buffer solution was flowed into the flow cell. The acceptor and donor intensities, $I_A(t)$ and $I_D(t)$, were recorded by sample scanning confocal microscopy at various stages of the reaction correspondingly, and the donor and acceptor images were analyzed. For each immobilized hairpin, an apparent FRET efficiency, E_A , was determined as follows:

$$E_A(t) = \frac{I_A(t)}{I_A(t) + I_D(t)}. \quad [1]$$

By measuring E_A for each hairpin, at various times, t , after introducing the complementary Cy5-hairpin solution FRET trajectories (Fig. 3A) were recorded to monitor the instantane-

ous distance between the 5' end of the immobilized Cy3-TAR DNA hairpin and the 3' end of the Cy5 hairpins.

FRET trajectories for individual reacting pairs (Fig. 3A) show the previously reported behavior of exhibiting discrete switching at the time of annealing from a low FRET value due to an isolated Cy3-TAR DNA hairpin to a high value due to an annealed Cy3-TAR DNA/Cy5-cTAR pair. FRET is efficient for the annealed pair because of the close proximity of the 5' end of TAR DNA and the 3' end of cTAR. Previously reported histograms of the FRET from many hairpins at different times during annealing show the expected dual peaks corresponding to the two-state annealing reaction (17). Very few of the hairpins reveal reverse annealing (high-to-low FRET changes), indicating that the annealing reaction highly favors the full duplex product state. This also demonstrates that photobleaching (18–20), which is also manifested by a similar high-to-low FRET change, is not a significant complication in these experiments. Some hairpins do not anneal during the time period because of nonidealities such as unlabeled cTAR and clustering or imperfect immobilization. Because of these imperfections, the mean FRET value as a function of time (Fig. 3B) does not perfectly reflect the true FRET changes because it reaches an asymptotic value of 0.86, whereas the E_A of the annealed form is ≈ 1 . Fig. 3C portrays the number of surviving reactant hairpins N_R (green curve) and the number of annealed product N_P (blue curve) pairs, respectively. These were determined by counting the number of hairpins that were below/above an E_A threshold of 0.4, as described in ref. 17.

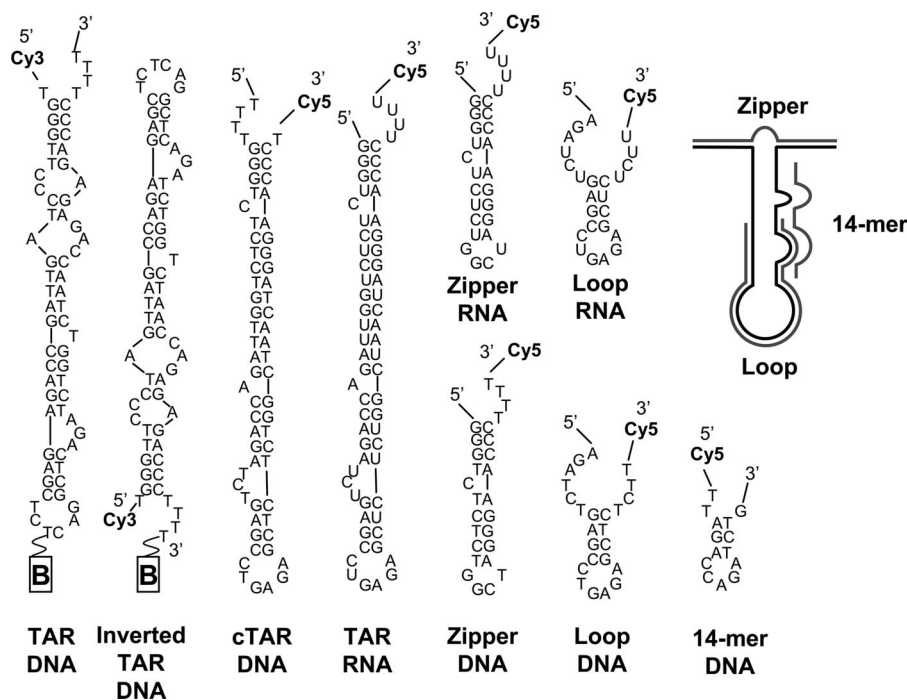


Fig. 2. Structures of various oligonucleotides used in this study. The secondary structures were predicted by the program mfold (www.bioinfo.rpi.edu/applications/mfold/dna/form1.cgi) (21).

The second and third columns in Fig. 3 correspond to annealing experiments with shorter DNA oligonucleotides that are targeted for “zipper” (L1L2 stem loops) and “loop” [L4, hairpin loop (HL)] regions of TAR DNA, as shown in Fig. 2. SMS data on annealing of both targeted oligonucleotides show evidence of reversible annealing that leads at later times to an equilibrium distribution of annealed and unannealed TAR. For example, the individual E_A trajectories show much more high-to-low FRET transitions than the TAR DNA/cTAR case. The (E_A) curves and the number of reactant and product data are also consistent with an equilibrium mixture at long times, with an apparent dissociation constant, K_d , of ≈ 10 nM and ≈ 16 nM for the zipper and loop DNA, respectively. One can estimate K_d from the $\approx 70\%$ and $\approx 60\%$ annealing percentage at 25 nM concentration for zipper and loop DNA, respectively. The annealed adducts of TAR DNA with the target oligonucleotides are arguably models for intermediates in the annealing reaction of full-length cTAR or TAR RNA and, indeed, in minus-strand transfer itself. We envision that the annealed form of TAR DNA with zipper is a model for the putative “Z” nucleation complex in Fig. 1, and that, in turn, the annealed adduct of TAR DNA with the loop oligonucleotide is a model for the “L” nucleation complex in Fig. 1. To simplify the nomenclature in this article, the equilibrium form of the annealed adduct of two nucleic acids will be denoted as follows, nucleic-acid-1/nucleic-acid-2, e.g., TAR DNA/zipper DNA. The annealing of TAR DNA with TAR RNA, zipper RNA, and loop RNA are more difficult to study accurately because of their higher tendency to form aggregates and stick to surfaces but generally exhibit similar kinetic behavior to the DNA oligonucleotides. As an example, the fourth column of Fig. 3 shows the kinetics of TAR DNA/zipper RNA annealing.

To characterize the nucleic acid rearrangement pathways available to the TAR DNA/targeted-oligonucleotide adducts, we subjected these models for nucleation complexes to a sequence of solutions containing buffer only, buffer plus NC, and NC plus cTAR. Typical results are shown in Fig. 4 for the loop DNA oligonucleotide. In the first time epoch of the experiment,

immobilized TAR was exposed to a loop DNA plus NC solution, leading to an annealing equilibrium. This was followed by a period in which the loop DNA plus NC solution was rapidly replaced with a buffer-only solution. The major effect of the buffer-only period was to freeze the concentration of the TAR/loop DNA adduct, even though the equilibrium constant strongly favors dislocated adducts in the absence of oligonucleotides in solution. In contrast, when NC was added to the solution (in the third epoch), the concentration of the adduct decreased relatively rapidly and continuously.

These data, therefore, demonstrate that NC not only catalyzes the forward annealing process but also catalyzes the reverse annealing process. This is expected according to microscopic reversibility for an NC-chaperoned process. Because NC interacts more strongly with single-stranded DNA than with double-stranded DNA, the combined NC effects strongly suggest that the transition state for the annealing reaction possesses more “single-stranded character” than the reactants, products, and even stable intermediates along the reaction path. This is qualitatively consistent with the proposed “Z” nucleation complex structure in Fig. 1. The final epoch in Fig. 4 involves an NC-promoted strand displacement of loop DNA by cTAR. This step in the sequence is a simple assay on the “activity” of the immobilized TAR hairpins, allowing for a validation of the entire procedure. Because efficient cTAR annealing was observed, it is unlikely that the TAR DNA hairpins were damaged or poorly immobilized by the programmed sequence of reagents. Very similar results were observed for the annealing of TAR DNA to zipper DNA, zipper RNA, and loop RNA.

Various observables and derived kinetic parameters for the annealing reaction of TAR DNA with the various nucleotides are listed in Table 1. Some clear trends are apparent in the data. For example, NC is clearly required for both the annealing and reverse annealing reactions to be rapid. In addition, the reverse annealing of the full-length oligonucleotides (cTAR and TAR RNA) is much slower than that of the short oligonucleotides, consistent with the idea that the annealed adduct of the TAR

Table 2. Summary of strand-displacement experiments

| Reaction sequence |
|--|
| Efficient strand displacement |
| Cy3-TAR/Cy5-zipper DNA + Cy5-cTAR |
| Cy3-TAR/Cy5-loop DNA + Cy5-cTAR |
| Cy3-TAR/Cy5-zipper RNA + Cy5-cTAR |
| Cy3-TAR/Cy5-loop RNA + Cy5-cTAR |
| Cy3-TAR/Cy5-14-mer DNA + cTAR |
| Inefficient strand displacement |
| Cy3-TAR/cTAR + Cy5-cTAR |
| Cy3-TAR/cTAR + Cy5-loop DNA |
| Cy3-TAR/cTAR + Cy5-cTAR + Cy5-14-mer DNA |

The annealing and replacement experiments were run in buffer containing 0.2 mM Mg^{2+} and 889 nM NC, 25 nM Cy5-zipper/loop nucleotide, and Cy5-cTAR DNA with the exception that the Cy5-14-mer DNA measurement was run with 50 nM Cy5-14-mer DNA and 2.5 nM unlabeled cTAR.

adducts of TAR DNA with short oligonucleotides, efficient strand displacements of the short oligonucleotide by another oligonucleotide were observed.

Further insights into the annealing mechanism were obtained by a different type of application of strand displacement, involving a short Cy5-labeled DNA oligonucleotide that is complementary to L3L4 (see 14-mer in Fig. 2). We used this 14-mer DNA as a “dynamic probe” for base pairing in the TAR DNA L3L4 region during the irreversible annealing of cTAR (Fig. 5). Because of the small number of base pairs in the TAR/14-mer adduct, its reverse annealing rate is very rapid. This was demonstrated by the single-molecule FRET trajectories in Fig. 5 *Upper*. Starting with a TAR DNA sample with no NC (epoch I), a solution of NC and Cy5-labeled 14-mer was added at the beginning of epoch II. Complete annealing was observed within the mixing time of the flow system, followed by rapid reversible on-off events in E_A trajectories due to rapid annealing/reverse annealing. The rapid NC-induced annealing is also reflected in the rapid rise of the mean FRET as a function of time curve (Fig. 5 *Lower*, epoch II). The most interesting part of Fig. 5 is the epoch III. At the beginning of epoch III, cTAR DNA was added to the NC and Cy5-labeled 14-mer solution, and a rapid irreversible displacement of the 14-mer by cTAR was observed at the usual time scale for TAR DNA/cTAR annealing. The fact that the irreversible annealing of nonlabeled cTAR DNA with TAR occurs with a concomitant displacement of the 14-mer is highly consistent with the hypothetical mechanism in Fig. 1, which assumes that full annealing occurs soon after the rate-limiting nucleation step.

Although the main features of the SMS data are well explained by the mechanism in Fig. 1, certain small but discernable features in the data suggest that the actual mechanisms may be somewhat more complex. For example, consider the interruption of the annealing equilibrium of the TAR DNA/zipper DNA adduct with a buffer-only washout step, as shown in Fig. 6. As expected from the mechanism in Fig. 1; the population of the adduct decayed only very slowly after the buffer entered the cell; i.e., the reverse annealing step requires NC to occur rapidly. The E_A trajectories also exhibit the expected underlying behavior; i.e., very few transitions between the low and high FRET levels after the buffer solution enters the sample cell. However, unexpectedly, immediately after the TAR/zipper DNA adduct was exposed to a buffer-only solution, a small but statistically significant drop was observed in the number of TAR DNA/zipper DNA adducts (N_P). A corresponding, unexpected small decrease in (E_A) was also observed. Both effects were reproduced in several trials. We tentatively assign the small, rapid drop in N_P to rapid reverse annealing of a conformational substate of the

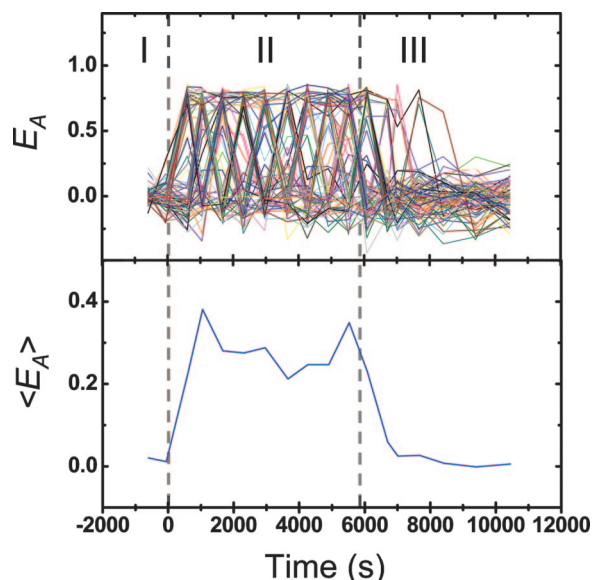


Fig. 5. Room-temperature, single-molecule E_A trajectories (*Upper*) and ensemble mean E_A (*Lower*) during the annealing reaction of Cy5-14-mer DNA annealed to Cy3-TAR DNA and then replaced by nonlabeled cTAR DNA. Three time epochs during the reaction are plotted: I, no annealing occurred in the presence of 50 nM Cy5-14-mer DNA only; II, reversible annealing reaction occurred in the presence of 50 nM Cy5-14-mer DNA and 889 nM NC; and III, the annealed Cy5-14-mer DNA was displaced by nonlabeled cTAR DNA in the presence of 2.5 nM nonlabeled cTAR DNA, 50 nM Cy5-14-mer DNA, and 889 nM NC. All reactions were run in the presence of 0.2 mM Mg^{2+} .

TAR/zipper adduct that is only partially annealed and, as a result, can be washed out by the incoming buffer solution. A good prospect for this substate is a “one-arm” annealed form of

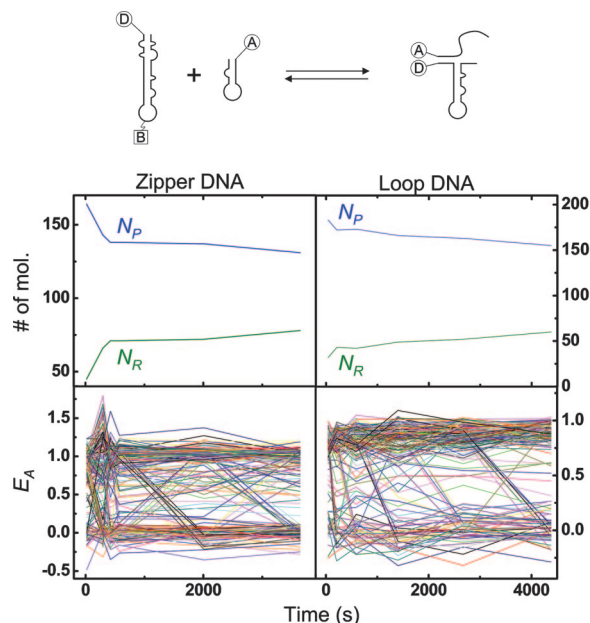


Fig. 6. Comparison between single-molecule measurements on buffer washout (0.2 mM Mg^{2+}) after immobilized Cy3-TAR DNA plus Cy5-zipper (*Left*) and immobilized inverted Cy3-TAR DNA plus Cy5-loop (*Right*) DNA annealing reaction. (*Upper*) Number of annealed (blue) and unannealed molecules during washout. (*Lower*) Single-molecule E_A trajectories. The equation shows a hypothetical scheme for the formation of a one-arm annealed TAR DNA/zipper DNA adduct.

the TAR DNA/zipper DNA adduct, as outlined in the equation at the top of Fig. 6. The “one-arm” annealed form is analogous to the previously reported rapidly reversible annealing of TAR DNA with a 13-mer short DNA oligonucleotide (5), which is complementary to only one arm of the “Y” form of TAR. This nonideality does not appear to be a factor for the TAR DNA/loop DNA adduct or for the full-length TAR DNA/cTAR reaction itself. Of course, all of the above observations are subject to our time resolution (>120 sec). The faster events beyond the time resolution will be missed, and the actual mechanism could be more complex.

Conclusions

An SMS approach has been developed for analyzing the mechanism of protein-induced nucleic acid rearrangements that involve multiple oligonucleotides and are highly heterogeneous and complex. The approach involves exposing one of the oligonucleotides (which is immobilized) to a sequence of solutions containing the complementary oligonucleotide, other target oligonucleotides, buffer only, and the chaperone protein in various combinations. This procedure effectively drags the nucleic acid/protein systems from reactants through key intermediates and finally toward the rearranged products while monitoring the conformational states and dynamics of the system with single-molecule FRET. Here, this sequence has been applied to investigate the NC protein-chaperoned annealing of TAR DNA to cTAR DNA/TAR RNA, which is an *in vitro* model for the minus-strand transfer step in

HIV-1 reverse transcription. The results strongly suggest that the nucleation event for annealing of transactivation response region TAR DNA to cTAR DNA involves base pair formation in different regions of TAR DNA. In addition, the results clearly demonstrate that NC induces reversible annealing at various stages along the reaction path of the annealing reaction.

Experimental Methods

SMS data were recorded by repetitive confocal scanning imaging as described in refs. 5 and 17. HIV-1 NC was synthesized as described in ref. 5. Various functionalized DNA hairpins (all purchased from TriLink BioTechnologies, San Diego, CA) and RNA hairpins (purchased from Dharmacon, Lafayette, CO) were used without further purification as described in ref. 5. TAR DNA was immobilized on the coverslip of an assembled flow chamber. Three syringe pumps delivered three solutions, NC, target complementary hairpins (containing Mg^{2+}), and buffer solution (containing buffer A and Mg^{2+}), separately. All of the solutions contained buffer A [40 mM NaCl/25 mM Hepes, pH 7.3/glucose oxygen scavenger system (5)].

We thank Dr. George Barany, Dr. Daniel G. Mullen, and Ms. Brandie J. Kovaleski (all of the University of Minnesota, Minneapolis) for chemical synthesis of NC. This work was supported by National Institutes of Health Grants GM65818 (to P.F.B.) and GM65056 (to K.M.-F.), National Institutes of Health postdoctoral National Research Service Award GM073534 (to C.F.L.), and the Welch Foundation (P.F.B.).

1. Levin JG, Guo J, Rouzina I, Musier-Forsyth K (2005) *Prog Nucleic Acid Res Mol Biol* 80:217–286.
2. Darlix J-L, Lapadat-Tapolsky M, de Rocquigny H, Roques BP (1995) *J Mol Biol* 254:523–537.
3. Rothwell PJ, Berger S, Kensch O, Felekyan S, Antonik M, Wohrl BM, Restle T, Goody RS, Seidel CAM (2003) *Proc Natl Acad Sci USA* 100:1655–1660.
4. Hong MK, Harbron EJ, O'Connor DB, Guo J, Barbara PF, Levin JG, Musier-Forsyth K (2003) *J Mol Biol* 325:1–10.
5. Liu H-W, Cosa G, Landes CF, Zeng Y, Mullen DG, Barany G, Musier-Forsyth K, Barbara PF (2005) *Biophys J* 89:3470–3479.
6. Cosa G, Harbron EJ, Zeng Y, Liu H-W, O'Connor DB, Eta-Hosokawa C, Musier-Forsyth K, Barbara PF (2004) *Biophys J* 87:2759–2767.
7. Cosa G, Zeng Y, Liu H-W, Landes CF, Makarov DE, Musier-Forsyth K, Barbara PF (2006) *J Phys Chem B* 110:2419–2426.
8. Hargittai MRS, Gorelick RJ, Rouzina I, Musier-Forsyth K (2004) *J Mol Biol* 337:951–968.
9. Urbaneja MA, Wu M, Casas-Finet JR, Karpel RL (2002) *J Mol Biol* 318:749–764.
10. Williams MC, Rouzina I, Wenner JR, Gorelick RJ, Musier-Forsyth K, Bloomfield VA (2001) *Proc Natl Acad Sci USA* 98:6121–6126.
11. Williams MC, Gorelick RJ, Musier-Forsyth K (2002) *Proc Natl Acad Sci USA* 99:8614–8619.
12. Stoylov SP, Vuilleumier C, Stoylova E, De Rocquigny H, Roques BP, Gerard D, Mely Y (1997) *Biopolymers* 41:301–312.
13. Le Cam E, Coulaud D, Delain E, Petitjean P, Roques BP, Gerard D, Stoylova E, Vuilleumier C, Stoylov SP, Mely Y (1998) *Biopolymers* 45:217–229.
14. Lapadat-Tapolsky M, De Rocquigny H, Van Gent D, Roques B, Plasterk R, Darlix JL (1993) *Nucleic Acids Res* 21:831–839.
15. Stoylov SP, Stoylova E, Todorov R, Schmiedel P, Thunig C, Hoffmann H, Roques BP, Le Cam E, Coulaud D, Delain E, *et al.* (1999) *Colloids Surf A* 152:263–274.
16. Fisher RJ, Fivash MJ, Stephen AG, Hagan NA, Shenoy SR, Medaglia MV, Smith LR, Worthy KM, Simpson JT, Shoemaker R, *et al.* (2006) *Nucleic Acids Res* 34:472–484.
17. Liu H-W, Zeng Y, Landes CF, Kim YJ, Zhu Y, Ma X, Vo M-N, Musier-Forsyth K, Barbara PF (2007) *Proc Natl Acad Sci USA* 14:5261–5267.
18. Widengren J, Schwillle P (2000) *J Phys Chem A* 104:6416–6428.
19. Fuereder-Kitzmueller E, Hesse J, Ebner A, Gruber HJ, Schuetz GJ (2005) *Chem Phys Lett* 404:13–18.
20. Sabanayagam CR, Eid JS, Meller A (2005) *J Chem Phys* 123:224708.
21. Zuker M (2003) *Nucleic Acids Res* 31:3406–3415.